

Droplet microfluidic technology for single-cell high-throughput screening

Eric Brouzes^{a,b,1}, Martina Medkova^a, Neal Savenelli^a, Dave Marran^a, Mariusz Twardowski^a, J. Brian Hutchison^a, Jonathan M. Rothberg^a, Darren R. Link^a, Norbert Perrimon^{b,c}, and Michael L. Samuels^a

^aRainDance Technologies, Lexington, MA 02421; and ^bGenetics Department, Harvard Medical School and ^cHoward Hughes Medical Institute, Boston, MA 02115

Edited by Noel A. Clark, University of Colorado, Boulder, CO, and approved June 2, 2009 (received for review March 31, 2009)

We present a droplet-based microfluidic technology that enables high-throughput screening of single mammalian cells. This integrated platform allows for the encapsulation of single cells and reagents in independent aqueous microdroplets (1 pL to 10 nL volumes) dispersed in an immiscible carrier oil and enables the digital manipulation of these reactors at a very high-throughput. Here, we validate a full droplet screening workflow by conducting a droplet-based cytotoxicity screen. To perform this screen, we first developed a droplet viability assay that permits the quantitative scoring of cell viability and growth within intact droplets. Next, we demonstrated the high viability of encapsulated human monocytic U937 cells over a period of 4 days. Finally, we developed an optically-coded droplet library enabling the identification of the droplets composition during the assay read-out. Using the integrated droplet technology, we screened a drug library for its cytotoxic effect against U937 cells. Taken together our droplet microfluidic platform is modular, robust, uses no moving parts, and has a wide range of potential applications including high-throughput single-cell analyses, combinatorial screening, and facilitating small sample analyses.

cell encapsulation | viability assay | lab-on-a-chip | emulsion | optical coding

Droplet-based microfluidic approaches present a paradigm for screening, providing increased throughputs, reduced sample volumes and single-cell analysis capabilities. Droplet microfluidics uses a 2-phase system, in which each assay is compartmentalized in an aqueous microdroplet (1 pL to 10 nL) surrounded by an immiscible oil. The advantages of this droplet-based technique include the physical and chemical isolation of droplets eliminating the risk of cross-contamination, the fast and efficient mixing of the reagents that occurs inside droplets, the ability to digitally manipulate droplets at a very high-throughput, the ability to incubate stable droplets off-chip and reintroduce them into the microfluidic environment for further processing and analysis, and the absence of moving parts [such as chip-integrated valves (1) or pumps]. In addition, because a small number of cells can be analyzed in discrete droplets, this technology is particularly suitable for working with cells of limited availability, such as stem cells or primary cells from patients.

Previously, important steps have been made to develop specific components required to perform droplet-based manipulations, including cell encapsulation (2–8), droplet merging (9–13), droplet mixing (14, 15), on-chip incubation (16), droplet sorting (17), and introduction of multiple compounds (18). However, each of these droplet manipulations has been demonstrated as separate modules that have not been assembled into an integrated biological assay. In addition, direct quantitative analysis of mammalian cells inside intact droplets that would require on-chip staining and thus a more complex integration of droplet modules, has not been shown. Finally, there have been no reported demonstrations using stable premade optically

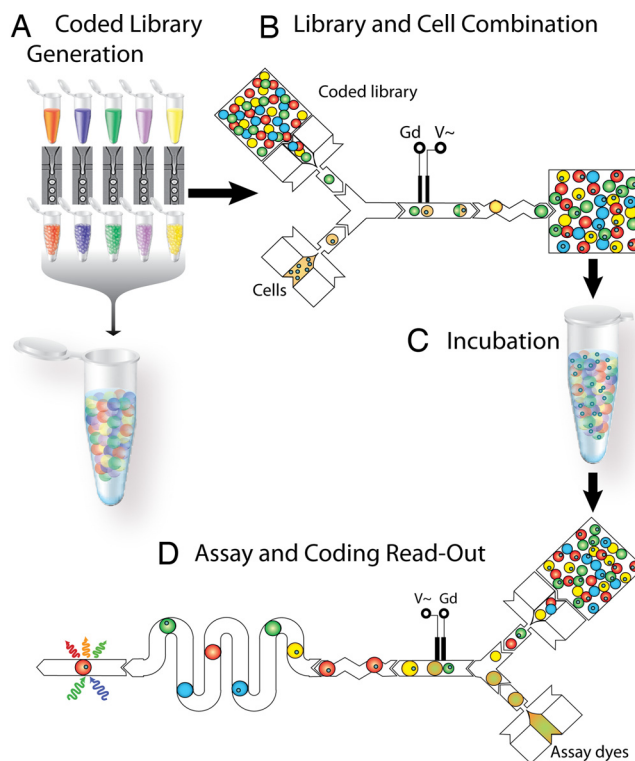


Fig. 1. Droplet screening workflow. The droplet screen has 4 steps. (A) A reformatting step to emulsify compound-code pairs and pool them into a droplet library. (B) Merging each library member with one of the cell-containing droplets that are continuously generated. Hence, each cell droplet has a specific composition defined by the compound droplet it has merged with. (C) Incubation. (D) Merged droplets are reinjected into an assay chip to identify each compound via their code and assess their specific effect on cells.

encoded droplet libraries, which are required for performing very high-throughput screens in the droplet format.

Here, by combining an on-chip cell viability assay and the automated generation of coded droplet libraries, we were able to develop a fully integrated droplet-based workflow for conducting a mammalian cell cytotoxicity screen at a very high-throughput. The development of the on-chip viability assay served 2 purposes. First, it permitted analysis of the overall utility and biocompatibility of the droplet format, by allowing direct

Author contributions: E.B., J.M.R., D.R.L., N.P., and M.L.S. designed research; E.B. and N.S. performed research; E.B., M.M., D.M., M.T., and J.B.H. contributed new reagents/analytic tools; E.B. analyzed data; and E.B. and M.L.S. wrote the paper.

The authors declare no conflict of interest.

This article is a PNAS Direct Submission.

¹To whom correspondence may be addressed: E-mail: brouzese@raindancetech.com or ebrouzes@genetics.med.harvard.edu.

This article contains supporting information online at www.pnas.org/cgi/content/full/0903542106/DCSupplemental.

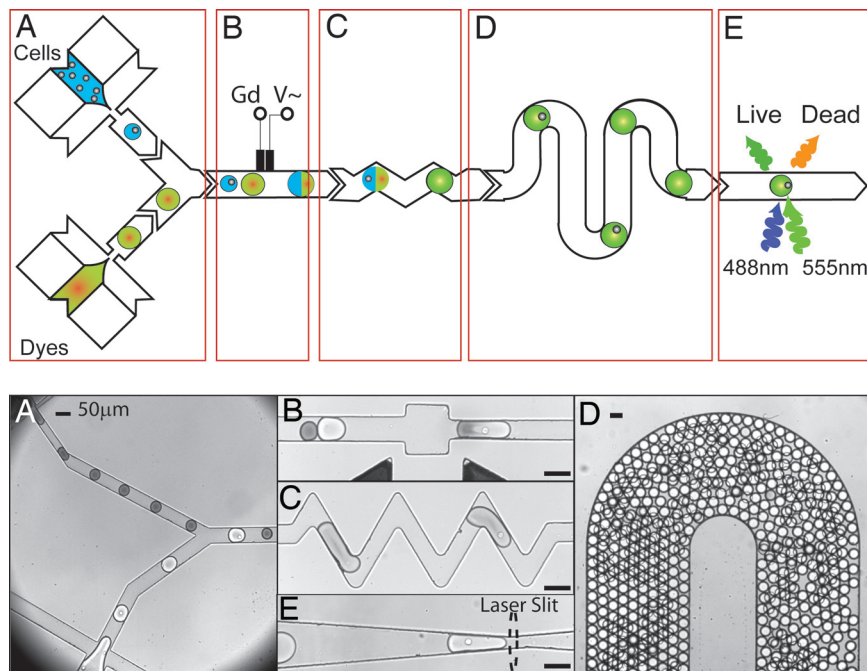


Fig. 2. Development of an on-chip viability assay. The viability assay chip integrated a series of 5 modules that had been optimized for analysis of cell viability. These modules sequentially manipulated droplets to conduct a viability assay on a single chip. (A) A set of 2 nozzles encapsulated cells and live/dead fluorescent dyes respectively. The fork enabled the interdigitation of the streams resulting in cell-containing droplets alternating with dye-containing droplets (100 μm deep channels). (B) A fusion module that delivered an AC field permitted electrically-controlled merging of pairs of dye-containing droplets and cell-containing droplets (100 μm deep). (C) A mixing module facilitated rapid and thorough mixing of cells with dyes (100 μm deep). (D) A delay line optimized cell staining by enabling on-chip incubation of the droplet for 15 min (260 μm deep). (E) A detection module confined droplet laterally and vertically to collect the fluorescent signals excited with a laser slit (100 μm deep). Live cells and dead cells were scored with Calcein-AM and Sytox Orange, respectively.

measurement of the viability of encapsulated cells. Second, it enabled cytotoxicity screening capabilities that are important in cancer research to either assess drug cytotoxicity or to screen cancer cells for therapeutic targets via synthetic lethality (19). This droplet workflow is generic and could be used with different types of libraries (e.g., DNA, siRNA, drug), fluorescent assay read-outs, or additional droplet manipulation modules.

Results

Droplet Screening Work-Flow. A droplet screening workflow (Fig. 1) involves 4 steps: (i) the drug library is formatted using the library generation chip into a droplet emulsion with each member uniquely coded with an optical label; (ii) each droplet library member is combined with a cell-containing droplet on a merge chip; (iii) the combined emulsion is incubated for cell treatment; and (iv) the emulsion is reinjected into the assay chip, where each droplet's fluorescence is measured for both assay and drug coding readouts. As a prerequisite to using the droplet workflow to conduct a cytotoxicity screen on mammalian cells, we first developed an integrated viability assay and used it to demonstrate the survival of encapsulated cells over a period of several days.

Development of the Integrated On-Chip Viability Assay Chip. We successfully developed a fully integrated droplet viability assay to interrogate cells within intact droplets using a standard fluorescent assay (see *Methods*). The assay sequentially performs a series of tasks by integrating 5 different droplet modules into a single chip: (i) a generation and reinjection module, with 1 nozzle for encapsulating the viability fluorescent dyes into droplets and a second nozzle for encapsulating cells or reinjecting cell emulsions (Fig. 2A and *Movie S1*); (ii) a module to merge droplet pairs includes an expansion region and a pair of electrodes that delivers an electric field to control pairwise coalescence (Fig. 2B and *Movie S2*); (iii) a serpentine mixing module

to rapidly trigger reactions (14, 15) (Fig. 2C and *Movie S3*); (iv) a delay line to allow on-chip enzymatic reactions to develop for 15 min (Fig. 2D and *Movie S4*); and (v) a detection module that elongates each droplet for consistent interrogation of every cell (Fig. 2E and *Movie S5*). Interrogation of each droplet's fluorescence was accomplished using laser line illumination and detection with photomultiplier tubes (PMTs) (Figs. 2E and 3A). Individual droplet signals decompose into a plateau that corresponds to the homogeneous droplet signal overlaid by a narrow peak that corresponds to a cell signal (Fig. 3B).

For this study, we used a flow-focusing nozzle (20, 21) to encapsulate monocytic U937 cells into 700 pL ($\approx 110 \mu\text{m}$) droplets at a rate of 100 droplets/s. Droplets were stabilized with a fluorinated surfactant that was selected to optimize cell viability (see *Methods*). Cell encapsulation follows a Poisson distribution that defines the droplet occupancy statistics (2, 5, 6), and resulted here in approximately one-third of the droplets being empty and one-third containing a single-cell.

From a fluidics perspective, a number of design parameters constrain the integration of different modules into a single device, including the need to optimize the nozzle dimensions to achieve the appropriate droplet sizes and frequencies, and a requirement to minimize back-pressure across the entire chip. The impact of nozzle design on droplet parameters was experimentally established and optimized in a few iterations (21–23). On-chip incubation presented a more difficult challenge, as strategies to increase droplet residence time by lengthening the channels also proportionally increase the pressure drop (24). This issue was solved with the use of delay-lines that have large cross-section channels that allow longer droplet incubation times while limiting back-pressure (24). We used a 3-layer lithography process to allow for the generation and manipulation of droplets in shallow channels and droplet incubation in deeper channels (Fig. S1C).

factant (36) to stabilize the droplets against coalescence while ensuring good biocompatibility of the interface when used with Pluronic F68.

After collection into 5-mL glass syringes, most of the oil was removed, and a 0.2- μm sterile Puradisc filter (Whatman) was inserted. The emulsions were stored in a standard incubator (37 °C, 5% CO₂), with the filter tip in contact with Dulbecco-PBS for buffering purpose. For cell growth experiments, images were taken during encapsulation and were used to count cell occupancy for the 0 h time points (ImageJ).

Viability and Cytotoxicity Experiments. Live and dead cells were scored with Calcein-AM and Sytox Orange (Invitrogen), while fluorescein (Invitrogen) was added at 0.1 μM to outline the droplets (Fig. 3B). The live-dead assay was conducted either with the encapsulation oil formulation (RainDance Technologies) with a fluorosurfactant (Zonyl-FSO, 1.3% wt; Dupont) added to the dye solution, or with a fluorinated PEG surfactant (37) in F oil (RainDance Technologies), with no notable difference.

For specificity and sensitivity experiments, live cells and dead cells were scored separately. Dead cells were prepared by incubation in 70% ethanol at 4 °C overnight. For sensitivity experiments, cells were prestained before on-chip scoring with Qdot 655 wheat germ agglutinin (Invitrogen). For the mixture experiments, the ratios of live and dead cells were measured at the end of the experiment by scoring cells going out of the injection vial. The viability chip operation was described in the main text.

The chip dimensions were: Nozzle for reinjecting the cell emulsion 80 μm wide \times 100 μm deep, nozzle for the dye solution encapsulation 100 μm wide \times 100 μm deep; the merge module was 340 μm wide, 320 μm long, and 100 μm deep; the mixing module consists of 9 U-turns that were 52.5 μm wide and 177 μm long with an angle of 60 °; the incubation line was 600 μm wide \times 260 μm deep and 1.5 m long; finally the detection module was 30 μm wide, 50 μm long, and 100 μm deep.

Data Acquisition and Analysis. A 488-nm laser (Picarro) and a 565-nm laser (Coherent) were focused into the channels through achromat and cylindrical

lenses (Edmund Optics). Fluorescence emissions were collected with a set of filters (535–40 nm, 617–73 nm, 710–40 nm; Semrock) and photomultiplier tubes (Hamamatsu). Fluorescence detection was driven at 100 kHz by a custom data-acquisition system (Labview; National Instruments) that also allowed signal processing and statistical analysis. Three thresholds were used to identify droplets, live cells, and dead cells. A collection of parameters was measured, and each cell peak was linked to droplet parameters (number of cells, size, and code).

Drug Library. Mitomycin C (Sigma) was mixed with the coding dye Alexa Fluor 680 R-phycoerythrin (Invitrogen) and diluted in RPMI before encapsulation. A custom-built library reformatting system was used to prepare each library. Each member was systematically encapsulated from a 96-well microtiter plate by being dispensed into a library generation chip. The members were collected into a vial, and the library was mixed before use. The layout of the fluidics chip consisted in a simple nozzle (80 μm wide \times 50 μm deep) and 2 outlets, of which 1 was used for collection (see Fig. S1A). The drug concentrations were encapsulated into 200 pL (73 μm) droplets by using 250 $\mu\text{L/h}$ flow-rate for the aqueous phase and 1250 $\mu\text{L/h}$ flow-rate for the oil phase.

Drug Library and Cells Combination. The combination chip layout comprised a set of 2 nozzles (Fig. S1B). One nozzle (60 μm wide and 100 μm deep) was used to space the library droplets, the other nozzle (80 μm wide and 100 μm deep) was used to encapsulate cells into 700 pL (\approx 110 μm) droplets. Both streams were collated before entering a merging module where they were combined as pairs. A short incubation-line (600 μm \times 0.24 m) assured optimal droplet stability before collection.

ACKNOWLEDGMENTS. We thank Phenix-Lan Quan, Yves Charles, Jeffrey Branciforte, Yue Suo, Haakan Joensson, Michael Weiner, Wolfgang Hinz, Bernard Mathey-Prevot, Chris Bakal, and RainDance Technologies for technical support and useful discussions. This work was supported by Small Business Innovation Research, National Institutes of Health (SBIR-NIH) Grant 5R43HG003925–02. N.P. is an Investigator of the Howard Hughes Medical Institute.

- Unger MA, et al. (2000) Monolithic microfabricated valves and pumps by multilayer soft lithography. *Science* 288:113–116.
- Clausell-Tormos J, et al. (2008) Droplet-based microfluidic platforms for the encapsulation and screening of Mammalian cells and multicellular organisms. *Chem Biol* 15:427–437.
- Edd JF, et al. (2008) Controlled encapsulation of single-cells into monodisperse picoliter drops. *Lab Chip* 8:1262–1264.
- He M, et al. (2005) Selective encapsulation of single cells and subcellular organelles into picoliter- and femtoliter-volume droplets. *Anal Chem* 77:1539–1544.
- Huebner A, et al. (2007) Quantitative detection of protein expression in single cells using droplet microfluidics. *Chem Commun* 12:1218–1220.
- Koster S, et al. (2008) Drop-based microfluidic devices for encapsulation of single cells. *Lab Chip* 8:1110–1115.
- Luo C, et al. (2006) Picoliter-volume aqueous droplets in oil: Electrochemical detection and yeast cell electroporation. *Electrophoresis* 27:1977–1983.
- Sgro AE, Allen PB, Chiu DT (2007) Thermoelectric manipulation of aqueous droplets in microfluidic devices. *Anal Chem* 79:4845–4851.
- Ahn K, et al. (2006) Electrocoalescence of drops synchronized by size-dependent flow in microfluidic channels. *Appl Phys Lett* 88:264105.
- Chabert M, Dorfman KD, Viovy JL (2005) Droplet fusion by alternating current (AC) field electrocoalescence in microchannels. *Electrophoresis* 26:3706–3715.
- Link DR, et al. (2006) Electric control of droplets in microfluidic devices. *Angew Chem Int Ed Engl* 45:2556–2560.
- Niu X, Gulati S, Edel JB, deMello AJ (2008) Pillar-induced droplet merging in microfluidic circuits. *Lab Chip* 8:1837–1841.
- Priest C, Herminghaus S, Seemann R (2006) Controlled electrocoalescence in microfluidics: Targeting a single lamella. *Appl Phys Lett* 89:134101.
- Sarrazin F, et al. (2007) Mixing characterization inside microdroplets engineered on a microcoalescer. *Chem Eng Sci* 62:1042–1048.
- Song H, Chen DL, Ismagilov RF (2006) Reactions in droplets in microfluidic channels. *Angew Chem Int Ed Engl* 45:7336–7356.
- Song H, Tice JD, Ismagilov RF (2003) A microfluidic system for controlling reaction networks in time. *Angew Chem Int Ed Engl* 42:768–772.
- Ahn K, et al. (2006) Dielectrophoretic manipulation of drops for high-speed microfluidic sorting devices. *Appl Phys Lett* 88:024104.
- Boedicker JQ, Li L, Kline TR, Ismagilov RF (2008) Detecting bacteria and determining their susceptibility to antibiotics by stochastic confinement in nanoliter droplets using plug-based microfluidics. *Lab Chip* 8:1265–1272.
- McManus KJ, Barrett IJ, Nohui Y, Hieter P (2009) Specific synthetic lethal killing of RAD54B-deficient human colorectal cancer cells by FEN1 silencing. *Proc Natl Acad Sci USA* 106:3276–3281.
- Loscertales IG, et al. (2002) Micro/nano encapsulation via electrified coaxial liquid jets. *Science* 295:1695–1698.
- Anna SL, Bontoux N, Stone HA (2003) Formation of dispersions using “flow focusing” in microchannels. *Appl Phys Lett* 82:364–366.
- Thorsen T, Roberts RW, Arnold FH, Quake SR (2001) Dynamic pattern formation in a vesicle-generating microfluidic device. *Phys Rev Lett* 86:4163–4166.
- Ward T, Faivre M, Abkarian M, Stone HA (2005) Microfluidic flow focusing: Drop size and scaling in pressure versus flow-rate-driven pumping. *Electrophoresis* 26:3716–3724.
- Frenz L, Blank K, Brouzes E, Griffiths AD (2009) Reliable microfluidic on-chip incubation of droplets in delay-lines. *Lab Chip* 9:1344–1348.
- Kiss MM, et al. (2008) High-throughput quantitative polymerase chain reaction in picoliter droplets. *Anal Chem* 80:8975–8981.
- Gonzalez JE, Negulescu PA (1998) Intracellular detection assays for high-throughput screening. *Curr Opin Biotechnol* 9:624–631.
- Joensson HN, et al. (2009) Detection and analysis of low-abundance cell-surface biomarkers using enzymatic amplification in microfluidic droplets. *Angew Chem Int Ed Engl* 48:2518–2521.
- Cushing MC, Anseth KS (2007) Materials science. Hydrogel cell cultures. *Science* 316:1133–1134.
- Chabert M, Viovy JL (2008) Microfluidic high-throughput encapsulation and hydrodynamic self-sorting of single cells. *Proc Natl Acad Sci USA* 105:3191–3196.
- Fournier-Bidoz S, et al. (2008) Facile and rapid one-step mass preparation of quantum-dot barcodes. *Angew Chem Int Ed Engl* 47:5577–5581.
- Han M, Gao X, Su JZ, Nie S (2001) Quantum-dot-tagged microbeads for multiplexed optical coding of biomolecules. *Nat Biotechnol* 19:631–635.
- Pregibon DC, Toner M, Doyle PS (2007) Multifunctional encoded particles for high-throughput biomolecule analysis. *Science* 315:1393–1396.
- Melkko S, et al. (2007) Isolation of high-affinity trypsin inhibitors from a DNA-encoded chemical library. *Angew Chem Int Ed Engl* 46:4671–4674.
- Portney NG, et al. (2008) Length-based encoding of binary data in DNA. *Langmuir* 24:1613–1616.
- Siegel AC, et al. (2006) Cofabrication of electromagnets and microfluidic systems in poly(dimethylsiloxane). *Angew Chem Int Ed Engl* 45:6877–6882.
- Johnston KP, et al. (1996) Water-in-carbon dioxide microemulsions: An environment for hydrophiles including proteins. *Science* 271:624–626.
- Holtze C, et al. (2008) Biocompatible surfactants for water-in-fluorocarbon emulsions. *Lab Chip* 8:1632–1639.